WAVELET DOMAIN BOOTSTRAP FOR TESTING THE EQUALITY OF BIVARIATE SELF-SIMILARITY EXPONENTS

Herwig Wendt[1], Patrice Abry[2], Gustavo Didier[3]

[1] IRIT, CNRS (UMR 5505), Université de Toulouse, France.
[2] Univ Lyon, Ens de Lyon, Univ Claude Bernard, CNRS, Laboratoire de Physique, Lyon, France.
[3] Math. Dept., Tulane University, New Orleans, LA, USA.

ABSTRACT

Self-similarity has been widely used to model scale-free dynamics, with significant successes in numerous applications that are very different in nature. However, such successes have mostly remained confined to univariate data analysis while many applications in the modern "data deluge" era involve multivariate and dependent data. Operator fractional Brownian motion is a multivariate self-similar model that accounts for multivariate scale-free dynamics and characterizes data by means of a vector of self-similarity exponents (eigenvalues). This naturally raises the challenging question of testing the equality of exponents. Expanding on the recently proposed wavelet eigenvalue regression estimator of the vector of self-similarity exponents, in the present work we construct and study a wavelet domain bootstrap test for the equality of self-similarity exponents from one single observation (time series) of multivariate data. Its performance is assessed in a bivariate setting for various choices of sample size and model parameters, and it is shown to be satisfactory for use on real world data. Practical routines implementing estimation and testing are available upon request.

Index Terms— multivariate self-similarity, operator fractional Brownian motion, wavelet spectrum, bootstrap, hypothesis testing

1. INTRODUCTION

Context: univariate self-similarity. Self-similarity [1] provides a framework for describing and modeling scale-free dynamics. It has been widely used and lead to well-recognized successes in numerous real world applications that are very different in nature (cf., e.g., [2–4] and references therein). Fractional Brownian motion (fBm) is the only Gaussian stationary increment self-similar process [5]. It has often been used to describe real world data, and offers a robust and versatile model whose dynamics are mainly governed by a unique self-similarity parameter H. In practice, the estimation of the latter parameter is naturally the central challenge. Knowledge of H permits carrying out various classical signal processing tasks such as characterization, diagnosis, classification, detection, etc. It is now well documented and widely accepted that the wavelet transform provides efficient multiscale representations and allows for theoretically well-grounded, robust and accurate estimation of H [2, 6]. However, such successes have remained mostly limited to univariate analysis. Modern applications often involve several joint time series, which calls for adequate multivariate self-similarity modeling.

Related work: multivariate self-similarity. Recently, operator fractional Brownian motion (ofBm), a multivariate extension of fBm, was proposed as a model for multivariate self-similarity [7–10]. In particular, it allows multiple correlated fBm coordinate processes with possibly distinct self-similarity exponents H_m, $m = 1, \ldots, M$, and occurring in a non-canonical set of coordinates (mixing). A statistical procedure was recently devised for jointly estimating the vector of self-similarity exponents $\underline{H} = (H_1, \ldots, H_M)$ [4, 11, 12]. Based on multivariate wavelet representations and eigenvalue decompositions, the method was mathematically studied and shown to have satisfactory theoretical and practical performance. Its actual use on real world data naturally raises a crucial question for data analysis or experimental interpretation — *are all self-similarity exponents $(H_1, \ldots, H_M)$ different or identical?* This question has never been addressed, except in the restricted setting [13]. In addition, it should be noted that the design of hypothesis tests in multivariate self-similarity contexts has to cope with the notorious intricacy of asymptotic estimator covariance matrices [14]. This work aims to provide the first and preliminary answer to this question in the wavelet domain.

Goal, contributions and outline. By making use of wavelet eigenvalue-based estimation for $\underline{H}$, the present work devises, studies and assesses a bootstrap-type test for the hypothesis $H_1 = H_2$ starting from one single observation (time series) of bivariate data. For the reader's convenience, bivariate ofBm is briefly developed in Section 2. After recapping the wavelet eigenvalue regression estimator of $\underline{H}$, Section 3 defines the new bootstrap-based testing procedure. In Section 4, Monte Carlo experiments involving a large number of independent copies of ofBm show that the proposed method permits effective testing of the hypothesis $H_1 = H_2$ from a single observation (time series). The performance of the test is characterized with respect to sample size and model parameters, notably the self-similarity exponents $\underline{H}$ and the Pearson correlation of the data. OfBm synthesis and self-similarity exponent estimation and testing are carried out by means of newly designed MATLAB routines.

2. OPERATOR FRACTIONAL BROWNIAN MOTION

The ofBm model was introduced and developed in general settings in [7–10]. It is a natural multivariate extension of fBm consisting of a multivariate Gaussian self-similar process with stationary increments. For ease of exposition of the principle behind the bootstrap test, the presentation is restricted to a bivariate and time reversible setting [9].

Let $X \equiv \{B_{H_1}(t), B_{H_2}(t)\}_{t \in \mathbb{R}}$ be a pair of fBm components defined by their self-similarity exponents $\underline{H} = (H_1, H_2)$, $0 <$

$H_1 \leq H_2 < 1$ and a pointwise covariance matrix Σ_X with entries $(\Sigma_X)_{m,m'} = \sigma_m \sigma_{m'} \rho_{m,m'}$, where σ_1^2, σ_2^2 and $\rho_0 \equiv \rho_{1,2}$ are the variance of each component and their respective correlation coefficients. Let P be a 2×2, real-valued, invertible matrix. In this contribution, we consider the particular framework where (bivariate) ofBm is defined by

$$Y \equiv \{B_1^{H,\Sigma_X,P}(t), B_2^{H,\Sigma_X,P}(t)\}_{t \in \mathbb{R}} = P\{B_{H_1}(t), B_{H_2}(t)\}_{t \in \mathbb{R}}$$

(in short, $Y = PX$). Bivariate ofBm is well-defined if and only if
$\Gamma(2H_1 + 1)\Gamma(2H_2 + 1)\sin(\pi H_1)\sin(\pi H_2)$
$-\rho_0^2 \Gamma(H_1 + H_2 + 1)^2 \sin^2(\pi(H_1 + H_2)/2) > 0$, thus showing that $\underline{H}$ and ρ_0 cannot be selected independently [9].

Let $\underline{\underline{H}} = P\mathrm{diag}(\underline{H})P^{-1}$ be the so-named Hurst matrix parameter, where $\underline{H}$ correspond to the Hurst eigenvalues. Multivariate self-similarity, the key property of ofBm, reads as

$$\{B_1^{H,\Sigma_X,P}(t), B_2^{H,\Sigma_X,P}(t)\}_{t \in \mathbb{R}} \overset{\mathrm{fdd}}{=} \\ \{a^{\underline{\underline{H}}}(B_1^{H,\Sigma_X,P}(t/a), B_2^{H,\Sigma_X,P}(t/a))\}_{t \in \mathbb{R}}, \quad (1)$$

$\forall a > 0$, where $\overset{\mathrm{fdd}}{=}$ stands for the equality of finite dimensional distributions, and $a^{\underline{\underline{H}}} := \sum_{k=0}^{+\infty} \log^k(a)\underline{\underline{H}}^k/k!$. When the mixing matrix P is diagonal, namely, when we can set $P \equiv I$, the self-similarity relation (1) takes the simple form of component-wise self-similarity relations (see [15])

$$\{B_1^{H,\Sigma_X,I}(t), B_2^{H,\Sigma_X,I}(t)\}_{t \in \mathbb{R}} \overset{\mathrm{fdd}}{=} \\ \{a^{H_1}B_1^{H,\Sigma_X,I}(t/a), a^{H_2}B_2^{H,\Sigma_X,I}(t/a))\}_{t \in \mathbb{R}}. \quad (2)$$

3. ESTIMATING $\underline{H}$ AND TESTING $H_1 = H_2$

3.1. Wavelet based joint estimation of H_1 and H_2

In statistical practice, the central task is to estimate the Hurst eigenvalues $\underline{H} = (H_1, H_2)$ from a single time series Y. When P is diagonal, (2) suggests that H_1 and H_2 can be estimated independently using standard univariate methodologies [13, 15]. However, in the general framework of nondiagonal mixing (coordinates) matrices P, univariate estimation does not yield relevant results. Instead, a multivariate wavelet transform-based joint estimation procedure can be used, cf. [4, 11]; it is recalled next for the reader's convenience.

Multivariate wavelet transform. Let ψ_0 be an oscillating reference pattern with joint time and frequency localization, referred to as the mother wavelet and further characterized by its so-named number of vanishing moments N_ψ. The latter is a positive integer such that $\forall n = 0, \ldots, N_\psi - 1$, $\int_{\mathbb{R}} t^k \psi_0(t)dt \equiv 0$ and $\int_{\mathbb{R}} t^{N_\psi}\psi_0(t)dt \neq 0$. Let $\{\psi_{j,k}(t) = 2^{-j/2}\psi_0(2^{-j}t - k)\}_{(j,k) \in \mathbb{Z}^2}$ be the collection of dilated and translated templates of ψ_0 that forms an orthonormal basis of $\mathcal{L}^2(\mathbb{R})$.

The multivariate discrete wavelet transform (DWT) of the multivariate stochastic process $\{Y(t)\}_{t \in \mathbb{R}}$ is defined as $(D(2^j, k)) \equiv D_Y(2^j, k) = (D_{Y_1}(2^j, k), D_{Y_2}(2^j, k))$, $\forall k \in \mathbb{Z}$, $\forall j \in \{j_1, \ldots, j_2\}$, and $\forall m \in \{1, 2\}$: $D_{Y_m}(2^j, k) = \langle 2^{-j/2}\psi_0(2^{-j}t - k)|Y_m(t)\rangle$. For a detailed introduction to wavelet transforms, interested readers are referred to, e.g., [16].

Joint estimation of H_1, H_2. Let $S(2^j)$ denote the empirical wavelet spectrum defined as

$$S(2^j) = \frac{1}{n_j}\sum_{k=1}^{n_j} D(2^j, k)D(2^j, k)^*, \quad n_j = \frac{N}{2^j},$$

where N is the sample size. Let $\Lambda(2^j) = \{\lambda_1(2^j), \lambda_2(2^j)\}$ be the eigenvalues of the 2×2 matrix $S(2^j)$. The wavelet eigenvalue regression estimators $(\hat{H}_1, \hat{H}_2)$ of (H_1, H_2) are defined by means of weighted log-regressions across scales $2^{j_1} \leq a \leq 2^{j_2}$ [4, 11]

$$\hat{H}_m = \left(\sum_{j=j_1}^{j_2} w_j \log_2 \lambda_m(2^j)\right)/2 - \frac{1}{2}, \quad \forall m = 1, 2. \quad (3)$$

Estimation performance. It was shown theoretically in [4, 11] that $(\hat{H}_1, \hat{H}_2)$ constitute consistent estimators with asymptotic joint normality under mild assumptions. It was also shown that these estimators have very satisfactory performance for finite sample sizes. Their covariances decrease as a function of the inverse of the sample size and are approximately normal even for small sample sizes. It was further observed that the variances of $(\hat{H}_1, \hat{H}_2)$ do not significantly depend on the actual values of (H_1, H_2).

3.2. Testing $H_1 = H_2$

Test formulation. The need to understand and analyze the data structure and underlying stochastic mechanisms leads to the issue of deciding whether or not H_1 and H_2 are equal. In other words, it is of great practical interest to test the null hypothesis $H_1 = H_2$ against the alternative hypothesis $H_1 \neq H_2$. A natural choice of test statistic is $\hat{\delta} = \hat{H}_2 - \hat{H}_1$.

In view of the asymptotic joint normality of $(\hat{H}_1, \hat{H}_2)$, $\hat{\delta}$ can be modeled as a zero mean Gaussian random variable, with unknown variance. With the purpose of testing $\hat{\delta} = 0$ from a single realization of the process, we propose to estimate its unknown variance by a bootstrap procedure [17, 18].

Bootstrap in the multivariate wavelet domain. To approximate the distribution of $\hat{\delta}$, a bootstrap method in the multivariate wavelet domain can be constructed that preserves the joint covariance structure of the wavelet coefficients. To this end, rather than bootstrapping independently on the wavelet coefficients of each component, the *vectors* of coefficients $D(2^j, k)$, $k = 1, \ldots, n_j$, are used in a (circular) block-bootstrap procedure [19]. For each scale j, from the periodically extended samples $(D(2^j, 1), \ldots, D(2^j, n_j))$, R block bootstrap resamples $D_j^{*(r)} = (D^{*(r)}(2^j, 1), \ldots, D^{*(r)}(2^j, n_j))$, $r = 1, \ldots, R$, are generated by a drawing-with-replacement procedure of $\lceil \mathrm{card}(Y)/L_B \rceil$ overlapping blocks of fixed size L_B, $(D(2^j, k), \ldots, D(2^j, k + L_B - 1), k = 1, \ldots, n_j$. Then, for each resample $D_j^{*(r)}$, bootstrap estimates $S^{*(r)}(j)$ and $(\hat{H}_1^{*(r)}, \hat{H}_2^{*(r)})$ are computed. The standard deviation of $\hat{\delta}$ is then approximated by the square root of the variance estimated from the R bootstrap samples $\hat{H}_2^{*(r)} - \hat{H}_1^{*(r)}$ and labeled σ_δ^*.

Bootstrap test. The bootstrap test for $H_1 = H_2$, with significance level α, is then defined as

$$\begin{aligned} d_\alpha = 1: & \quad |\hat{\delta}| > \sigma_\delta^* t_{1-\frac{\alpha}{2}} \quad (H_1 = H_2 \text{ rejected}) \\ d_\alpha = 0: & \quad |\hat{\delta}| \leq \sigma_\delta^* t_{1-\frac{\alpha}{2}} \quad (H_1 = H_2 \text{ accepted}), \end{aligned} \quad (4)$$

where $t_\pi = F^{-1}(\pi)$ and F is the standard normal cumulative distribution function.

4. TEST PERFORMANCE ASSESSMENT

4.1. Monte Carlo simulation

Monte Carlo experiments are conducted to assess the validity of the multivariate bootstrap procedure and to quantify the performance of
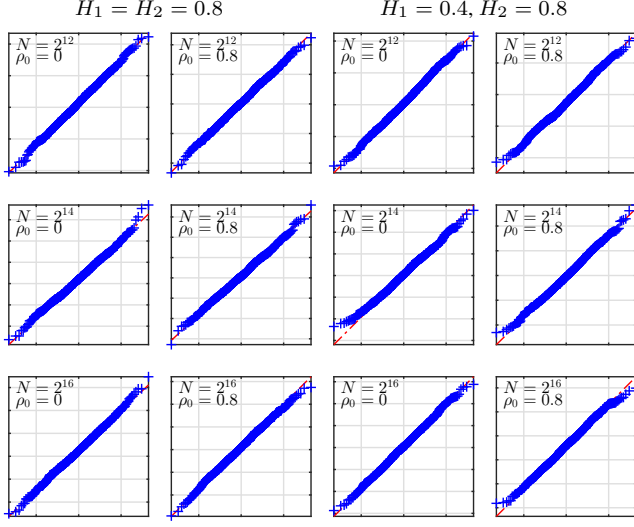
Fig. 1. **Gaussanity of estimates.** Quantile-quantile-plots against standard normal of estimates $\delta = H_2 - H_1$ under the null (left) and alternative (right) hypothesis, showing that estimates for δ are well modeled by a Gaussian distribution.
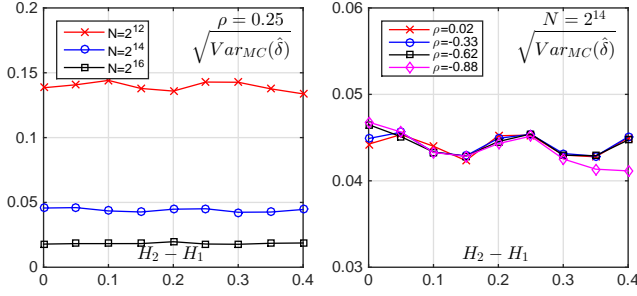

Fig. 2. **Standard deviation of $\hat{\delta}$** for several values of N (left) and ρ (right) as a function of $H_2 - H_1$.

the test. $N_{MC} = 1000$ independent realizations of synthetic bivariate ofBm of sizes $N \in \{2^{12}, 2^{14}, 2^{16}\}$ are subjected to the estimation procedure and test. Under the null hypothesis, ofBm parameters are set to $H_1 = H_2 = 0.8$. Under the alternative hypothesis, $H_2 = 0.8$ and $H_1 \in \{0.75, 0.7, \ldots, 0.45, 0.4\}$. The significance level (i.e., error of type 1) of the test is set to $\alpha = 0.05$. The test performance is reported for several correlation levels $\rho_0 \in \{-0.6, -0.4, 0, 0.4, 0.8\}$. The mixture matrix is set to $P = ((0.69\ 0.31)^T, (0.07\ -0.93)^T)$. For all these instances, asymptotic joint normality holds [4]. This leads to an effective correlation coefficient of $\rho \in \{0.25, 0.02, -0.33, -0.62, -0.88\}$ for the analyzed bivariate time series $Y = PX$. Other choices, not reported here, yield equivalent performance. For the analysis, we use least asymmetric Daubechies 3 wavelets (hence $L_B = 6$), $j_1 = 5$ and $j_2 = \{7, 9, 11\}$, and $R = 500$ bootstrap resamples.

4.2. Statistical properties of $\hat{\delta} = \hat{H}_2 - \hat{H}_1$

Monte Carlo experiments first enabled us to study the statistical properties of $\hat{\delta}$. Fig. 1 shows quantile-quantile plots of $\hat{\delta}$ against the standard normal distribution for several sample sizes, both when
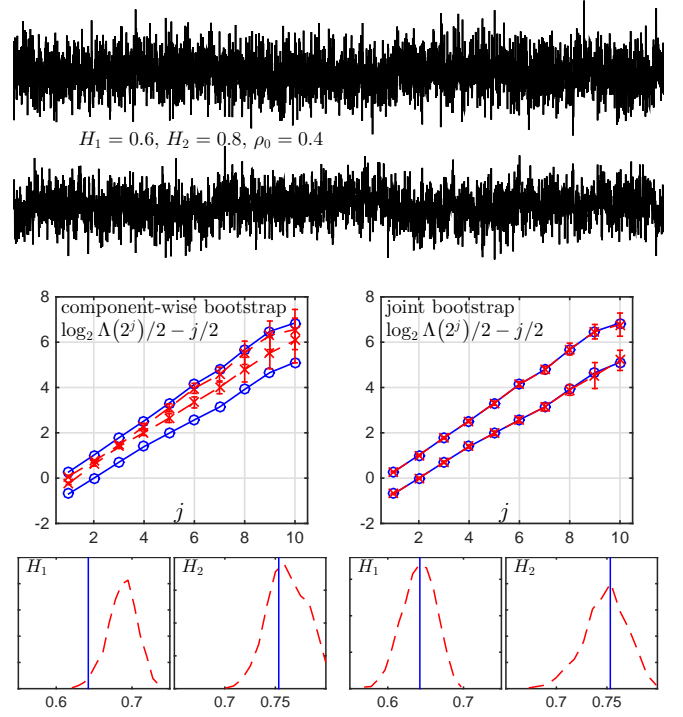

Fig. 3. **Bootstrap resampling.** <u>Top</u>: single realization of bivariate ofBm ($N = 2^{14}$). <u>Center</u>: log-scale diagrams of $\log_2 \lambda(S(j))$ (blue solid lines and circles) and for their bootstrap replica $\log_2 \lambda(S^*(j))$ (averages and standard 95% confidence intervals; red dashed lines and crosses) obtained by component-wise independent resampling (left) and by the joint resampling method (right). <u>Bottom</u>: corresponding estimates and bootstrap histograms for H_1, H_2.

$H_1 = H_2$ and $H_1 \neq H_2$. The plots clearly validate the normal approximation to the distribution of $\hat{\delta}$. Furthermore, Fig. 2 reports standard deviations of $\hat{\delta}$ estimated over Monte Carlo realizations, denoted $\sqrt{Var_{MC}(\hat{\delta})}$, as a function of $H_2 - H_1$, for several values for N and ρ. It clearly illustrates the fact that the variance of $\hat{\delta}$ does not depend on the values of H_1, H_2 or ρ, and decreases as $\sim \frac{1}{N}$ apart from border effects of the wavelet transform.

4.3. Multivariate bootstrap accuracy and relevance

Multivariate vs. univariate resampling. We illustrate the relevance of the proposed multivariate resampling strategy by comparing it with a bootstrap scheme that generates resamples of the wavelet coefficients $D_{Y_m}(2^j, k)$ *independently* for each component m, instead of vector-wise. In Fig. 3, the functions $\log_2 \Lambda(2^j)$ (blue lines) and their bootstrap replicas (averages and confidence intervals, red) are plotted, together with histograms of bootstrap estimates $\hat{H}_m^*$ for a single realization of bivariate ofBm, once for component-wise bootstrap (left), and once based on the multivariate resampling scheme (right). The empirical distribution obtained using the univariate bootstrap clearly fails to accurately estimate the distributions of $\log_2 \Lambda(2^j)_m$ and H_m, which stands in contrast to those obtained from the advocated multivariate resampling scheme.

Accuracy of bootstrap variance estimation. To shed more light on the accuracy of the proposed multivariate resampling strategy, in
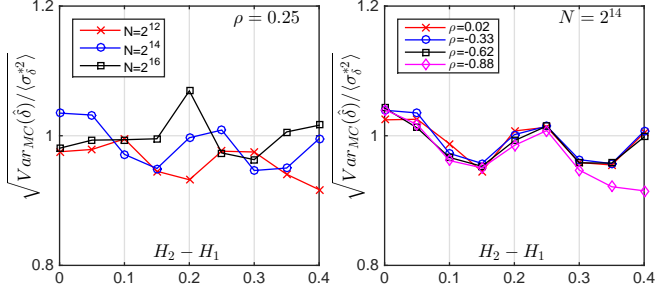
Fig. 4. **Bootstrap variance accuracy.** Ratio of Monte Carlo standard deviation and average bootstrap standard deviation estimates for several values for N (left) and ρ (right).
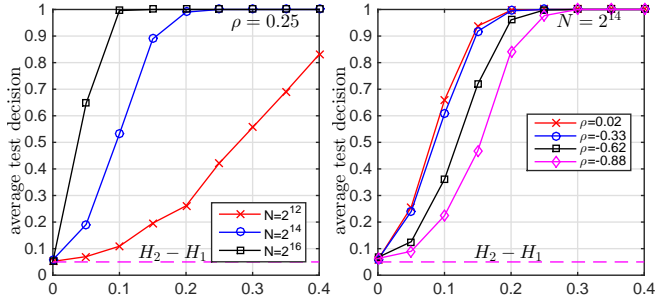

Fig. 5. **Test performance.** Average bootstrap decisions (for 1000 independent realizations) as a function of $H_2 - H_1$, for different levels of correlation $\rho \in \{-0.8, -0.4, 0, 0.4, 0.8\}$ (from left to right, respectively) and sample sizes $N \in \{2^{12}, 2^{14}, 2^{16}\}$: the leftmost points ($H_2 - H_1 = 0$) correspond to the null hypothesis and quantify the type 1 error of the test (for preset significance $\alpha = 0.05$, indicated by horizontal dashed line), the other points ($H_2 - H_1 > 0$) correspond to alternative hypotheses and quantify the test power.

Fig. 4 we report the ratios of the Monte Carlo variances $Var_{MC}(\hat{\delta})$ and averages (over Monte Carlo realizations) of the bootstrap variance estimators σ_δ^{*2} as a function of $H_2 - H_1$ and for several values for N and ρ. The results show that the bootstrap variance estimates are on average excellent, lying within a few percent of the true (Monte Carlo) variances, irrespective of sample size N, correlation level ρ, and specific values of H_1 and H_2.

4.4. Test performance

Test performance under the null hypothesis. Fig. 5 plots average (over 1000 independent realizations) test decisions for three different sample sizes N (left plot; $\rho = 0.25$) and several values for ρ (right plot; $N = 2^{14}$), for $H_2 = 0.8$ and various values for H_1. The leftmost points ($H_2 - H_1 = 0$) correspond to the null hypothesis, i.e., $H_1 = H_2 = 0.8$, under which the average test decisions ideally reproduce the significance level α. The results clearly show that in all situations (i.e., for all sample sizes N and correlation levels ρ), the average test decisions are very close to the preset value $\alpha = 0.05$. This indicates that the null distribution model used in (4), relying on asymptotic Gaussianity and bootstrap estimates of the unknown variance, is highly accurate.

Test performance under alternative hypotheses. The points to the right of $H_2 - H_1 = 0$ in Fig. 5 correspond to the average test decisions under the alternative hypothesis with $H_1 = 0.8$ and

$H_2 \in \{0.75, 0.7, \ldots, 0.45, 0.4\}$ (i.e., increasing δ); hence, they quantify the power of the test. The results were as follows. The test power increases both with the sample size and with the difference $H_2 - H_1$, as expected. Interestingly, the power of the test slightly decreases for increasing correlation ρ between the components of ofBm. This indicates that it is more difficult to identify the existence of two different values of H in data when the components are correlated. Nevertheless, the reported test powers should be satisfactory for most applications and enable, for instance, for $N = 2^{16}$ to detect a small difference of 0.05 between H_1 and H_2 with reasonable probability $> 65\%$ for $\rho = 0.25$ (and still $> 25\%$ for $N = 2^{14}$). Note that these sample sizes are common in applications such as Internet traffic modeling [20] and macroscopic brain activity analysis [21]. The test power could also be further increased by setting the onset scale j_1 to a smaller value, which leads to a larger effective sample size. These results further suggest that the proposed bivariate estimation and test methods are effective in disentangling the mixed ofBm components (since, otherwise, the estimated values $\hat{H}_1$ and $\hat{H}_2$ would be close and the test power small).

Overall, the reported results show that the proposed testing procedure for the equality of pairs of scaling exponents of ofBm with nondiagonal mixing (coordinates) matrix is operational and effective, and can be readily applied to real world data.

5. CONCLUSIONS AND PERSPECTIVES

This work puts forward a new test for the equality of the self-similarity exponents H_1 and H_2 of ofBm with non-trivial mixing (coordinates) matrix, that is, for situations where classical univariate estimation procedures cannot be used. The testing procedure is constructed in the wavelet domain and relies on three original ingredients. First, it makes use of a sample wavelet eigenvalue regression approach for the accurate estimation of the self-similarity exponents (eigenvalues) in mixed components; second, the asymptotic joint normality for the corresponding estimators, established in [4, 11], is used; third, a multivariate nonparametric block bootstrap resampling scheme is devised that preserves the multivariate statistical structure of the (wavelet vector coefficients of the) data. A broad Monte Carlo study illustrates that the proposed procedure has satisfactory performance in detecting differences between H_1 and H_2 even at small sample sizes. In view of the notorious intricacy of asymptotic estimator covariance matrices in multivariate self-similarity frameworks, we provide an operational and effective procedure that can actually be applied to real world data. MATLAB code for the estimation and testing procedures (together with the ofBm synthesis procedure) is available upon request and published on the the authors' webpages.

Future methodological work includes the extension of the method to the testing of the equality of multiple self-similarity exponents H. This implies devising multiple hypotheses tests or a strategy that allows to estimate how many self-similarity parameters are actually different amongst the multiple estimates. Also, when the number of components increases while the sample size remains small (high dimension), the Gaussian approximation to the distribution of $\hat{\delta}$ might prove to be less accurate. Hence, instead of assuming a priori the normality of $\hat{\delta}$ and applying the bootstrap only in variance estimation, the distribution of the statistic itself could be estimated by means of the multivariate bootstrap procedure, which requires a modification of the final test formulation. Finally, the estimation and test procedures will be used in applications such as in macroscopic brain dynamics analysis of neuroscientific data.

6. REFERENCES

[1] G. Samorodnitsky and M. Taqqu, *Stable non-Gaussian random processes*, Chapman and Hall, New York, 1994.

[2] D. Veitch and P. Abry, "A wavelet-based joint estimator of the parameters of long-range dependence," *IEEE Transactions on Information Theory*, vol. 45, no. 3, pp. 878–897, 1999.

[3] H. Wendt, P. Abry, and S. Jaffard, "Bootstrap for empirical multifractal analysis," *IEEE Signal Processing Magazine*, vol. 24, no. 4, pp. 38–48, 2007.

[4] P. Abry and G. Didier, "Wavelet eigenvalue regression for n-variate operator fractional Brownian motion," *arXiv preprint arXiv:1708.03359*, 2017.

[5] B. B. Mandelbrot and J. W. van Ness, "Fractional Brownian motion, fractional noises and applications," *SIAM Reviews*, vol. 10, pp. 422–437, 1968.

[6] P. Flandrin, "Wavelet analysis and synthesis of fractional Brownian motion," *IEEE Transactions on Information Theory*, vol. IT-38, no. 2, pp. 910–917, 1992.

[7] M. Maejima and J. D. Mason, "Operator-self-similar stable processes," *Stochastic Processes and their Applications*, vol. 54, no. 1, pp. 139–163, 1994.

[8] J. D. Mason and Y. Xiao, "Sample path properties of operator-self-similar Gaussian random fields," *Theory of Probability & Its Applications*, vol. 46, no. 1, pp. 58–78, 2002.

[9] G. Didier and V. Pipiras, "Integral representations and properties of operator fractional Brownian motions," *Bernoulli*, vol. 17, no. 1, pp. 1–33, 2011.

[10] G. Didier and V. Pipiras, "Exponents, symmetry groups and classification of operator fractional Brownian motions," *Journal of Theoretical Probability*, vol. 25, pp. 353–395, 2012.

[11] P. Abry and G. Didier, "Wavelet estimation for operator fractional Brownian motion," *Bernoulli*, vol. 24, no. 2, pp. 895–928, 2018.

[12] G. Didier, H. Helgason, and P. Abry, "Demixing multivariate-operator self-similar processes," in *IEEE International Conference on Acoustics, Speech and Signal, Processing (ICASSP), Brisbane, Australia*, Brisbane, Australia, 2015, pp. 3671–3675.

[13] H. Wendt, G. Didier, S. Combrexelle, and P. Abry, "Multivariate Hadamard self-similarity: testing fractal connectivity," *Physica D*, vol. 356-357, pp. 1–36, 2017.

[14] P. Abry, G. Didier, and H. Li, "Two-step wavelet-based estimation for Gaussian mixed fractional processes," *arXiv preprint 1607.05167*, pp. 1–60, 2017.

[15] P.-O. Amblard and J.-F. Coeurjolly, "Identification of the multivariate fractional Brownian motion," *IEEE Transactions on Signal Processing*, vol. 59, no. 11, pp. 5152–5168, 2011.

[16] S. Mallat, *A Wavelet Tour of Signal Processing*, Academic Press, San Diego, CA, 1998.

[17] B. Efron, *The Jackknife, the Bootstrap, and Other Resampling Plans*, Society for Industrial and Applied Mathematics, Philadelphia, 1982.

[18] A. M. Zoubir and D. R. Iskander, *Bootstrap Techniques for Signal Processing*, Cambridge University Press, ISBN 0-521-83127-X, 2004.

[19] S. N. Lahiri, *Resampling Methods for Dependent Data*, Springer, New York, 2003.

[20] R. Fontugne, P. Abry, K. Fukuda, D. Veitch, K. Cho, P. Borgnat, and H. Wendt, "Scaling in Internet traffic: a 14 year and 3 day longitudinal study, with multiscale analyses and random projections," *IEEE/ACM Transactions on Networking*, vol. 25, no. 4, pp. 1–14, 2017.

[21] N. Zilber, P. Ciuciu, P. Abry, and V. Van Wassenhove, "Modulation of scale-free properties of brain activity in MEG," in *IEEE International Symposium on Biomedical Imaging (ISBI)*. IEEE, 2012, pp. 1531–1534.